Supporting Information:

Thickness-tunable Core-shell Co@Pt Nanoparticles Encapsulated in Sandwich-like Carbon Sheets as Enhanced Electrocatalyst for Oxygen Reduction Reaction

*Tao Xiang[1], Ling Fang[1], Jing Wan[2], Li Liu[1], Jiao Jiao Gao[1],Hai Tao Xu[1], Hui Juan Zhang[1], Xiao Gu[2] and Yu Wang**

[1]The State Key Laboratory of Power Transmission Equipment and System Security

[2]Department of Applied Physics, Chongqing University, 174 Shazheng Street, Shapingba District, Chongqing City, 400044, P.R. China.

*E-mail: wangy@cqu.edu.cn

Table S1. Compositions of sandwiched-like Co@Pt/C-1, Co@Pt/C-2 and Co@Pt/C-3 core-shell catalysts, determined by ICP-AES.

Composites	Experimental (ICP-AES) Co/Pt ratio
Co@Pt/C-1	90.22/9.78
Co@Pt/C-2	86.29/13.71
Co@Pt/C-3	84.34/15.66

Table S2. ORR activity date of Co@Pt core-shell structure or Pt_xCo_y alloy NPs from the previous literatures.

sample	Mass activity (A/mg_{Pt})	Specific activity (mA/cm^{-2})	ref
Sandwich-like Co@Pt/C core-shell	1.77	1.21	This work
Co@Pt core-shell	0.072	0.145	1
Core-shell-like Pt_3Co		0.14	2
Pt-coated Co nanowires	0.793	2.725	3
Co@Pt/C core-shell	0.05		4
Co@Pt core-shell	0.17	0.41	5
PtCoN/C	0.63	0.7	6
CNC Pt-Co/rGO		1.14	7
PtCo nanowires	0.2	1.6	8
Pt_3Co/C	0.15	0.18	9

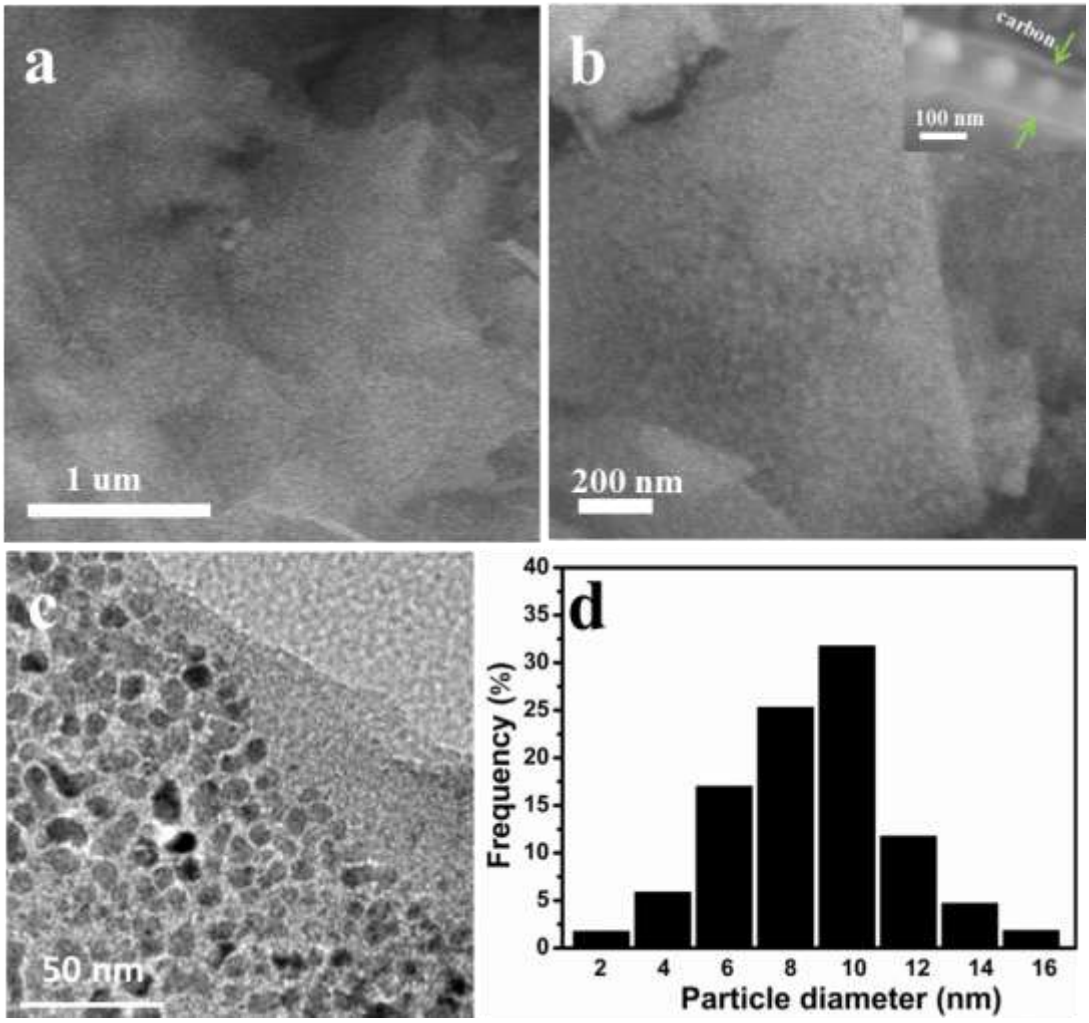

Figure S1. (a) (b) SEM images, (c) TEM image and (d) particle-size distribution of the sandwich-like Co/C NPs.

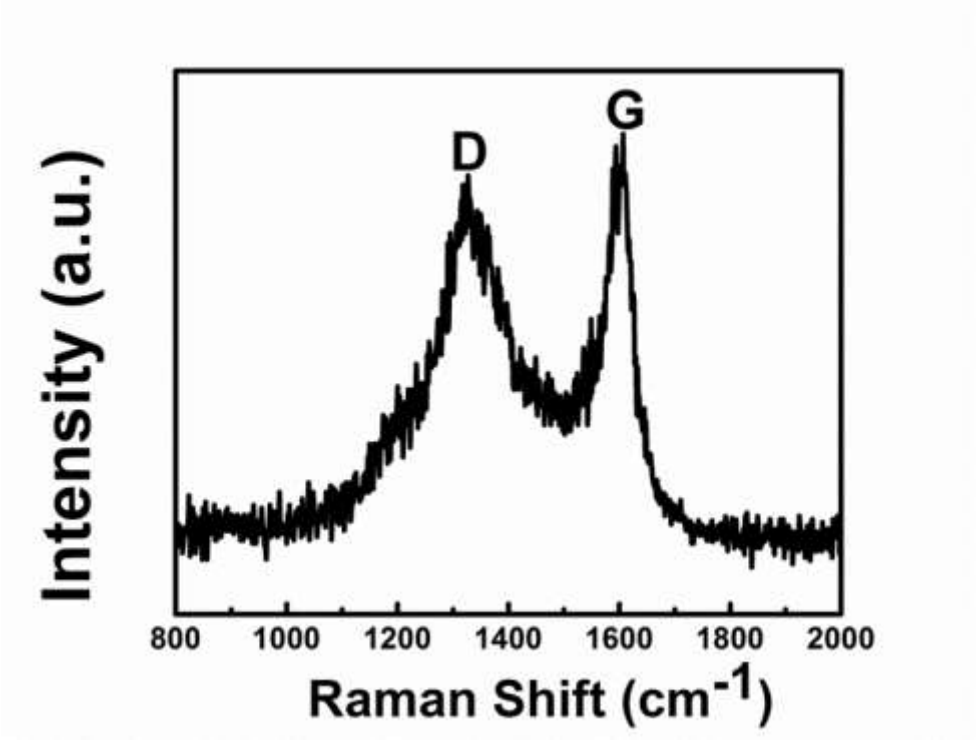

Figure S2. Raman spectrum to disclose the graphitization of sandwich-like Co@Pt/C-2 core-shell catalyst, implying the presence of well-graphitized carbon.

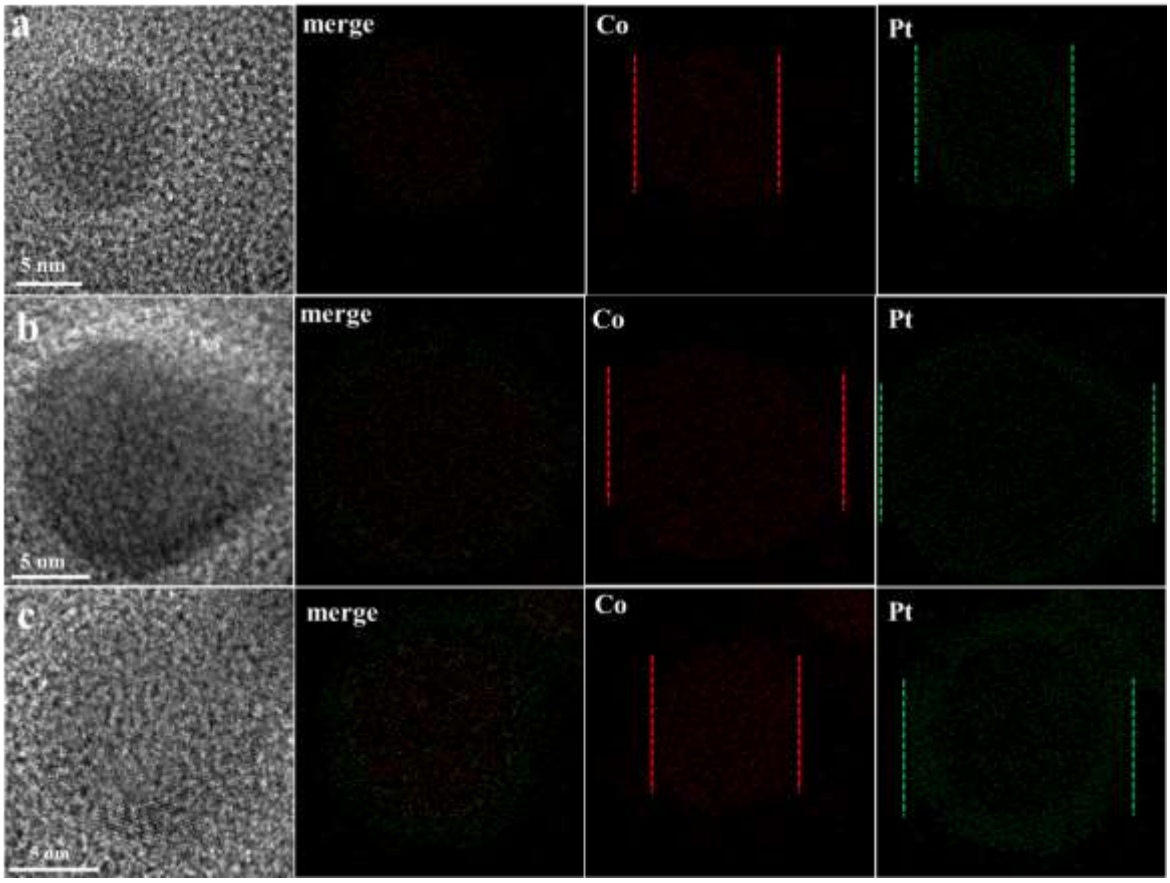

Figure S3. The HRTEM images and EDS elemental mappings of Co, Pt obtained for the single sandwich-like core-shell Co@Pt/C-1 (a), Co@Pt/C-2 (b) and Co@Pt/C-3 (c) catalysts.

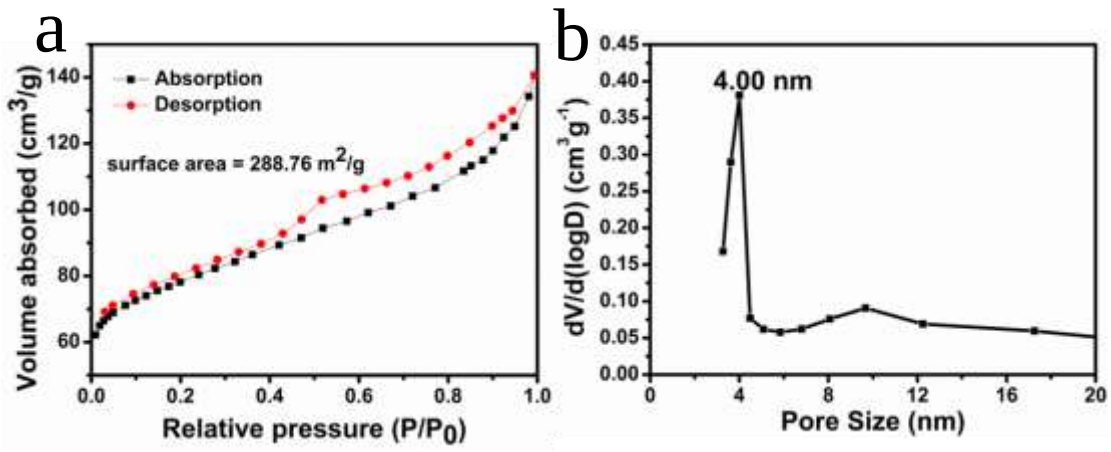

Figure S4. Nitrogen adsorption-desorption isotherm of the specific sandwiched structure to reveal the specific surface area (a) and corresponding pore size distribution (b) of sandwich-like Co@Pt/C-2 core-shell catalyst.

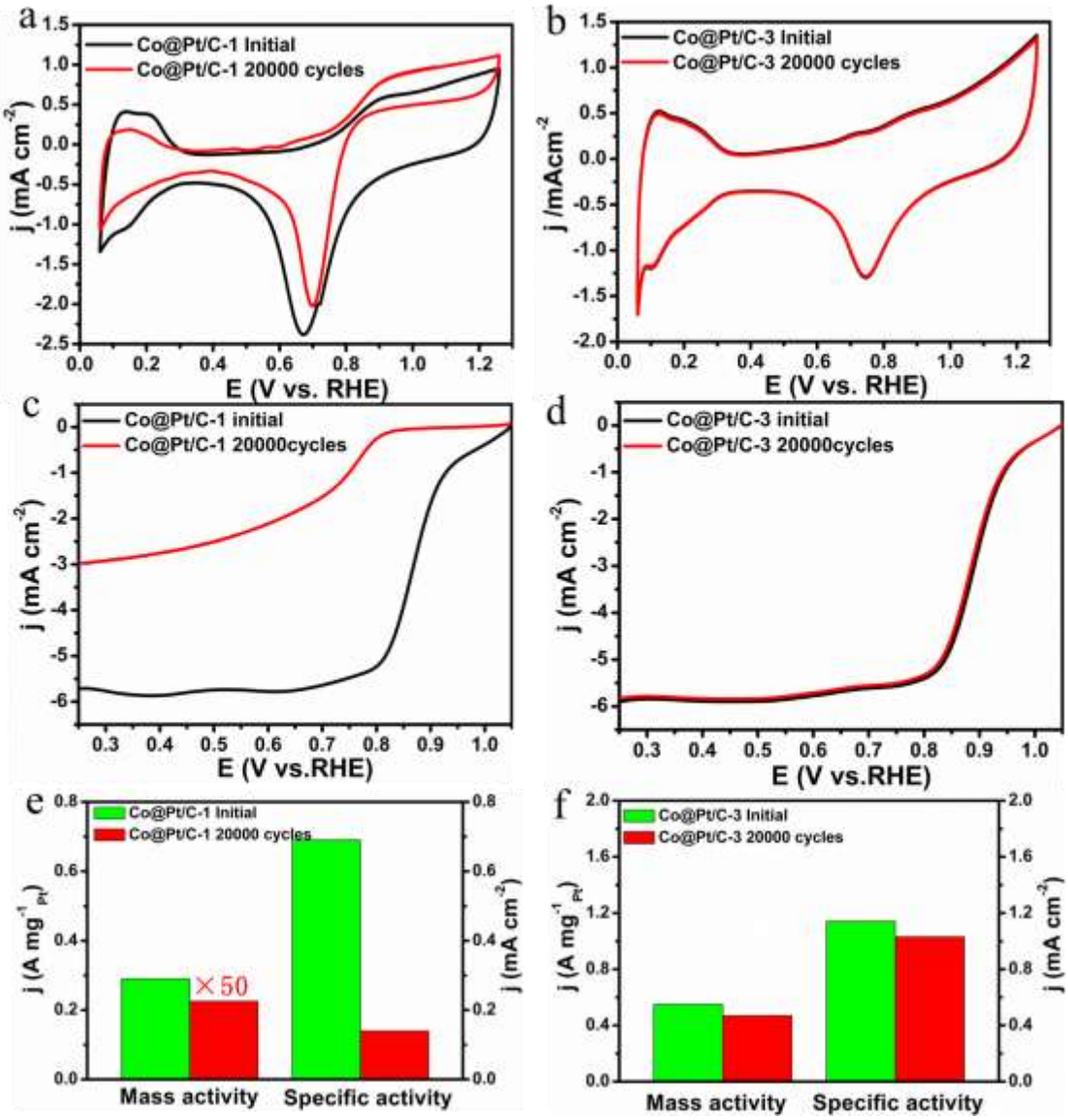

Figure S5. CV and ORR polarization curves of Co@Pt/C-1 (a,b) and Co@Pt/C-3 (c, d) before and after different potential cycles, respectively. (e) and (f) show the changes of mass activities and specific activities of Co@Pt/C-1 and Co@Pt/C-3 before and after different potential cycles, respectively.

Calculation details:

The ORR reaction pathways on the Co@Pt/C core-shell catalyst were computed. The dissociative mechanism of O_2 has been detailedly understand by Nørskov et al, and the four electron ORR pathway can be calculated by the following steps.[10]

$$O_2 + 4(H^+ + e^-) \rightarrow 2H_2O \quad (1)$$

$$O_2 + * \rightarrow O_2^* \quad (2)$$

$$O_2^* + e^- + H^+ \rightarrow OOH^* \quad (3)$$

$$OOH^* + (H^+ + e^-) \rightarrow O^* + H_2O \quad (4)$$

$$O^* + (H^+ + e^-) + H_2O \rightarrow OH^* + H_2O \quad (5)$$

$$OH^* + (H^+ + e^-) + H_2O \rightarrow 2H_2O \quad (6)$$

Where, the formula (1) is the total reaction of oxygen reduction, and formulae (2)-(6) are the elementary steps of oxygen reduction reaction.

The Gibbs free energy change for steps 3-6 can be calculated by following schemes.

$$\Delta G_1 = \Delta G(OOH) - \Delta G(O_2) + eU + \Delta G_{PH}$$

$$\Delta G_2 = \Delta G(O) - \Delta G(OOH) + eU + \Delta G_{PH}$$

$$\Delta G_3 = \Delta G(OH) - \Delta G(O) + eU + \Delta G_{PH}$$

$$\Delta G_4 = 0 - \Delta G(OH) + eU + \Delta G_{PH}$$

Where U was the potential of normal hydrogen electrode (NHE) at the standard conditions (T = 298.15 K, P = 1 bar, pH = 0). Here the $\Delta G(O_2)$ was set as 4.92 eV, which is difficult to calculate accurately by GGA-DFT.[11] The Gibbs free energies of OOH, O and OH were determined by the equation: $\Delta G = \Delta E + \Delta ZPE - T\Delta S$.

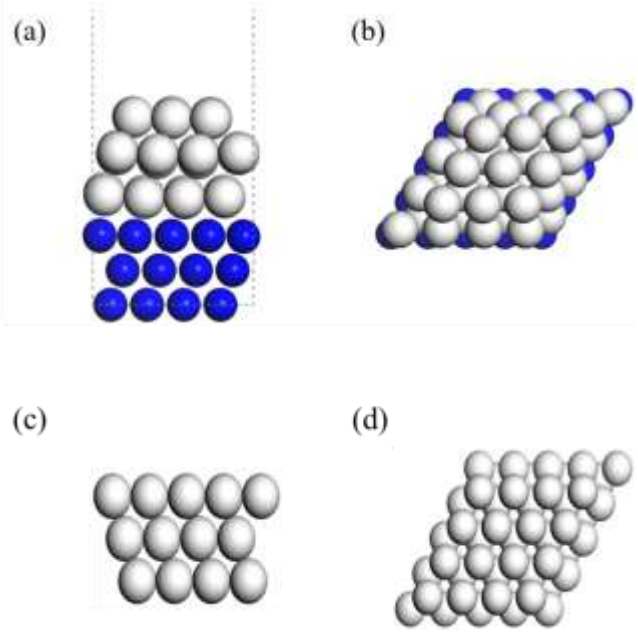

Figure S6. In the structures of Co@Pt/C core-shell structure and pure Pt, the white and blue balls are Pt atoms and Co atoms, respectively. (a) and (b) are the side view and top view of Co@Pt/C core-shell structure. (c) and (d) are the side view and top view of pure Pt.

Reference：

1. L. Wang, Z. Tang, W. Yan, Q. Wang, H. Yang and S. Chen, *J. Power Sources*, 2017, **343**, 458-466.
2. J.-H. Jang, J. Kim, Y.-H. Lee, I. Y. Kim, M.-H. Park, C.-W. Yang, S.-J. Hwang and Y.-U. Kwon, *Energy Environ. Sci.*, 2011, **4**, 4947.
3. S. M. Alia, S. Pylypenko, K. C. Neyerlin, D. A. Cullen, S. S. Kocha and B. S. Pivovar, *ACS Catal.*, 2014, **4**, 2680-2686.
4. R. Lin, C. Cao, T. Zhao, Z. Huang, B. Li, A. Wieckowski and J. Ma, *J. Power Sources*, 2013, **223**, 190-198.
5. D. A. Cantane, F. E. R. Oliveira, S. F. Santos and F. H. B. Lima, *Appl. Catal., B*, 2013, **136-137**, 351-360.
6. B. P. Vinayan and S. Ramaprabhu, *Nanoscale*, 2013, **5**, 5109-5118.
7. Y. Qin, X. Zhang, X. Dai, H. Sun, Y. Yang, X. Li, Q. Shi, D. Gao, H. Wang, N. F. Yu and S. G. Sun, *Small*, 2016, **12**, 524-533.
8. D. C. Higgins, R. Wang, M. A. Hoque, P. Zamani, S. Abureden and Z. Chen, *Nano Energy*, 2014, **10**, 135-143.
9. Y. Yu, H. L. Xin, R. Hovden, D. Wang, E. D. Rus, J. A. Mundy, D. A. Muller and H. D. Abruna, *Nano Lett.*, 2012, **12**, 4417-4423.
10. J. K. Nørskov, J. Rossmeisl, A. Logadottir, L. Lindqvist, J. R. Kitchin, T. Bligaard and H. Jónsson, *J. Phys. Chem. B*, 2004, **108**, 17886-17892.
11. M. Bajdich, M. Garcia-Mota, A. Vojvodic, J. K. Norskov and A. T. Bell, *J. Am. Chem. Soc.*, 2013, **135**, 13521-13530.